

Glutamine 151 Participates in the Substrate dNTP Binding Function of HIV-1 Reverse Transcriptase[†]

Stefanos G. Sarafianos, Virendra N. Pandey, Neerja Kaushik, and Mukund J. Modak*

Department of Biochemistry and Molecular Biology, UMD-New Jersey Medical School, Newark, New Jersey 07103

Received December 9, 1994; Revised Manuscript Received March 17, 1995[®]

ABSTRACT: In order to define the role of Gln151 in the polymerase function of HIV-1 RT, we carried out site-directed mutagenesis of this residue by substituting it with a conserved (Q151N) and a nonconserved residue (Q151A). Q151N exhibited properties analogous to those of the wild-type enzyme, while Q151A has severely impaired polymerase activity. The Q151A mutant exhibited a 15–100-fold reduction in k_{cat} with RNA [poly(rC) and poly(rA)] templates, while only a 5-fold reduction could be seen with the DNA [poly(dC)] template. Most interestingly, the affinity of the Q151A mutant for dNTP substrate remained unchanged with RNA templates, but a significant increase in K_m was noted with the DNA template. The binding affinity of Q151A for DNA remained unchanged, as judged by photoaffinity cross-linking. However, unlike the wild-type enzyme, the Q151A mutant failed to catalyze the nucleotidyl transferase reaction onto the primer terminus of the covalently immobilized template-primer. The enzyme showed profoundly altered divalent cation preference from Mg^{2+} to Mn^{2+} . These results strongly implicate Q151 of HIV-1 RT in the substrate dNTP binding function and possibly in the following chemical (catalytic) step. The effects of the mutation seem to be through Q151 of the p66 catalytic subunit, as p66_{WT}/p51_{Q151A} retains the wild-type kinetic constants and nucleotidyl transferase activity. In contrast, p66_{Q151A}/p51_{WT} is indistinguishable from Q151A (mutated in both subunits). A model of the ternary complex (enzyme–template-primer and dNTP) has been used to infer the possible mode by which Q151 may interact with the base moiety of the substrate as well as with Arg72, a residue present within the active site of HIV-1 RT.

The rapid emergence of human immunodeficiency virus (HIV-1) strains resistant to specific inhibitors has frustrated the efforts to control the spread of the acquired immunodeficiency syndrome. The resistance to inhibitors directed at the reverse transcriptase of HIV-1 (HIV-1 RT)¹ is thought to be due to mutations in this enzyme (Larder & Kemp, 1989; Larder et al., 1989a,b, 1991). It is therefore imperative that a thorough understanding of the catalytic mechanism of HIV-1 RT be achieved. The X-ray structure of HIV-1 RT (Jacobo-Molina et al., 1993; Kohlstaedt et al., 1992) has provided useful information regarding the tertiary folding pattern and general location of the various amino acids; however, a detailed mapping of the substrate binding site, a prerequisite for rational drug design, is still missing. With the exception of the three acidic residues (Asp110, Asp185, and Asp186), which are presumed to interact with the dNTP substrate by binding to the divalent cation required for the

polymerase reaction (Larder et al., 1987; Le Grice et al., 1991; Beard et al., 1994; Jacques et al., 1994), no other residue has been shown experimentally to participate in the substrate binding function of HIV-1 RT. The presence of the above mentioned three acidic residues in the catalytic center of the DNA polymerase class of enzymes, with functional implication in the binding of the metal–chelate form of dNTP, is now well established (Lowe et al., 1991; Polesky et al., 1990; Sawaya et al., 1994). Recently, a molecular modeling study in our laboratory indicated that the catalytic domains of HIV-1 RT and *Escherichia coli* DNA polymerase I, despite their weak sequence homology, contain a number of identical or similar residues that are spatially conserved in both the enzymes (Yadav et al., 1994). In the same study, Q151 of HIV-1 RT was proposed to be the residue corresponding to N845 of pol I, which has been suggested to be involved in the dNTP binding function (Polesky et al., 1990). Earlier, the role of Q151 was not fully recognized in three mutant screening studies, where Q151E (Boyer et al., 1994), Q151H (Larder et al., 1989b), or Q151N (Boyer et al., 1992) exhibited 30%, 30%, and 100% activities, respectively compared to the wild-type enzyme. Consequently, the role of Q151 was not fully investigated. In order to obtain experimental evidence in support of our speculation that Q151 may participate in the substrate binding function, we generated the Q151A and Q151N mutants by site-directed mutagenesis of codon 151. The mutants were cloned in high expression vectors, and the purified proteins were used to carry out a detailed comparative analysis of the properties of mutant and wild-type enzymes. The results of this investigation suggest that

[†]This research was supported in part by a grant from the National Institute of Allergy and Infectious Diseases (NIAID 26652).

* Address correspondence to this author at (telephone, 201 982-5515; Fax, 201 982-5594).

[®] Abstract published in *Advance ACS Abstracts*, May 1, 1995.

¹ Abbreviations: BSA, bovine serum albumin; dNTP, deoxynucleotide triphosphate; DTT, dithiothreitol; EDTA, ethylenediaminetetraacetic acid; foscamet or PFA, phosphonoformic acid; HEPES, *N*-(2-hydroxymethyl)piperazine-*N'*-2-ethanesulfonic acid; IMAC, immobilized metal affinity chromatography; KF, Klenow fragment; PP_i, pyrophosphate; poly(dC)•(dG)₁₅, poly(deoxycytidine)(deoxyguanosine)₁₅; poly(rA)•(dT)₁₅, poly(riboadenosine)(thymidine)₁₅; poly(rC)•(dG)₁₅, poly(ribocytidine)(deoxyguanosine)₁₅; RT, reverse transcriptase; SDS–PAGE, sodium dodecyl sulfate–polyacrylamide gel electrophoresis; TCA, trichloroacetic acid; TP, template-primer; WT, wild type; UV, ultraviolet. The kinetic nomenclature and constants used are according to Cleland (1963).

Q151 of HIV-1 RT, similar to N845 of *E. coli* DNA polymerase I, participates in the dNTP binding function and that mutation in the p66 subunit is responsible for the altered properties. Several additional catalytic properties of the Q151A mutant enzyme, such as alteration in the divalent cation preferences and pH optimum, were also uncovered. On the basis of the above results, a tentative model for the participation of Q151 in the prepolymerase ternary complex of HIV-1 RT/template-primer/dNTP has been proposed.

EXPERIMENTAL PROCEDURES

Materials

Restriction endonucleases, *Taq* DNA polymerase, and DNA-modifying enzymes were from Promega or Boehringer Mannheim while HPLC-purified dNTPs were obtained from Boehringer Mannheim. Sequenase and other DNA sequencing reagents were from U.S. Biochemicals. Mutagen-M13 in vitro mutagenesis kit was purchased from Bio-Rad laboratories. Expression vector pet-28a and expression strain BL21 (DE3) were obtained from Novagen. All other reagents were of the highest purity grade and were purchased from Fisher, Millipore Corp., Boehringer Mannheim, and Bio-Rad. Synthetic template-primers were purchased from Pharmacia and ^{32}P -labeled dNTPs and ATP were the products of Dupont/New England Nuclear Corp. Sequencing primers and oligonucleotides containing the desired mutational changes were purchased from Midland Certified Reagent, Dallas, TX, and were purified by electrophoresis followed by chromatography on Sep Pak (Millipore) C_{18} .

Methods

Reverse Transcriptase Activity Assay. Reverse transcriptase activity was assayed as reported previously (Basu et al., 1989). Assay solution contained 0.1 A_{260} units/mL homopolymeric TP, 0.02 mM $[\text{H}]$ dNTP (0.5 μCi /assay), 80 mM NaCl, 1 mM DTT, 50 mM HEPES, pH 7.8 (unless otherwise indicated), and 5 mM MgCl_2 . Typically, an aliquot containing approximately 50 ng enzyme (150 ng in the case of Q151A) was incubated in a final reaction volume of 0.1 mL at 37°. The reaction was initiated by the addition of MgCl_2 and terminated by the addition of 5% ice-cold TCA at 15 min. The TCA-precipitable materials were collected on Whatman GF/B filters and counted for radioactivity in a liquid scintillation counter, as described before (Basu et al., 1989).

Steady-State Kinetics of Polymerization. The kinetic studies were carried out as described previously (Majumdar et al., 1988), using homopolymeric poly(rA)•(dT)₁₅, poly(rC)•(dG)₁₅, or poly(dC)•(dG)₁₅ as template-primers and dTTP or dGTP as nucleotide substrates. K_{m} s for dNTP were determined at saturating template-primer concentrations (50 μg /mL), whereas K_{m} s for DNA were determined at saturating dNTP concentrations (0.15 mM). Velocities for each substrate concentration were fit to the Michaelis–Menten equation, and least squares lines were drawn for the Lineweaver–Burk plots. K_{m} s and V_{max} s were calculated graphically; k_{cat} s were calculated from the equation $V_{\text{max}} = k_{\text{cat}}[\text{E}]$. Inhibition constants were determined from Dixon plots, as described previously (Majumdar et al., 1988). Kinetic experiments were performed at least twice, and values were averages of at least duplicate samples. Activity determination and kinetic studies at various pHs were

performed as above, with the exception of using glycine for higher pH buffers.

RNase H Activity Assay. The assays were performed essentially as described elsewhere (Basu et al., 1989). The assay solution contained 2–5 μM (as total nucleotides) poly- $[\text{H}](\text{rA})\cdot\text{poly}(\text{dT})$ (100 000 dpm/assay), 80 mM NaCl, 5 mM MgCl_2 , 3% glycerol, 50 mM HEPES, pH 8.0, 0.1 mg/mL BSA, and 100 ng of enzyme. Reactions were carried out at 37 °C and processed as described for the reverse transcriptase activity assays.

Construction of Expression Plasmids and in Vitro Mutagenesis. DNA manipulations were carried out according to standard protocol (Ausubel et al., 1987). We used the prokaryotic expression plasmid pET-28-a (Novagen) for expression of recombinant HIV-1 RT. The full-length (1.68 kb) coding sequence of HIV-1 RT66 was amplified from the DE-52 plasmid (Sharma et al., 1992) using polymerase chain reaction. The thermal cycle parameters were as described before (Pandey et al., 1993). The *Nde*I and *Bam*HI sites were introduced at the 5' and 3' ends, respectively, during the amplification. The PCR product was cloned in pET-28a to construct pET-28a-RT66. Similarly, the 1.32 kb p51 coding region (codon 1–440) was amplified from DE-52 by PCR, and the *Nhe*I and *Sac*I sites were introduced at the 5' and 3' ends, respectively, along with a TAA stop codon at the 3' end of the coding sequence. The amplified fragment was cloned in pET-28a to construct pET-28a-RT51. The *Xba*I and *Sac*I of pET-28a-RT51 encoding the polymerase domain of HIV RT was subcloned in bacteriophage M13mp18 and was used as the template for site-directed mutagenesis. The mutagenesis protocol using uracil-containing template was essentially as described by Kunkel et al. (1985). After ascertaining the mutation in M13 by DNA sequencing, the desired mutation was introduced by subcloning the appropriate fragment in the pET-28a-RT cassette. Subsequently it was introduced into *E. coli* BL21 (DE3) for expression. Induction by IPTG was performed as described before (Pandey et al., 1994b).

Overexpression and Isolation of HIV-1 RT and Its Mutant Derivatives. The expression and isolation of proteins were performed as described by Sharma et al. (1992). The purified proteins from pET-28a-RT66 were predominantly in the p66/p66 homodimer form (Chattopadhyay et al., 1992). Purified proteins from the pET-28a-RT66 and pET-28a-RT51 systems were more than 98% pure, as judged by SDS–PAGE. The different combinations of chimeric heterodimers were prepared by reconstitution of the separate subunits. Cell lysates of the different bacterial strains were mixed at the appropriate ratios, essentially following the protocol described by Le Grice et al. (1991). The molar ratio of the subunits in the chimeric heterodimers was 1:1 (Le Grice et al., 1991). Protein concentrations were determined by using the Bio-Rad colorimetric kit as well as by spectrophotometric measurements using $\epsilon_{278} = 6.32 \times 10^4 \text{ M}^{-1} \text{ cm}^{-1}$ (Setlow et al., 1972).

Determination of the Rate Constants for the First Nucleotide Incorporation by Wild-Type and Mutant Enzymes. Rates of incorporation of the first nucleotide ($[\text{H}]$ dTMP) were measured using the 18/47 template-primer (TP). The standard assay mixture contained 150 nM TP, 400 nM enzyme, 50 mM HEPES, pH 8.0, 80 mM NaCl, and 20 μM $[\alpha\text{-}^{32}\text{P}]\text{dTTP}$. Reactions were initiated at 25 °C by the addition of MgCl_2 (5 mM final), and aliquots were withdrawn at 5–10-s intervals. The incorporation of radiolabeled

substrate was determined by acid precipitation. The first-order rate of single nucleotide incorporation in E-template-primer was measured from the slope of the first-order plot of $\ln\{[E-TP]_{\text{remaining}}/[E-TP]_{\text{initial}}\}$ vs time. The "initial" concentration of E-TP was estimated from the amount of dNTP incorporated in E-TP at prolonged incubation (30 min), assuming 1:1 stoichiometry. The amount of E-TP remaining unused at time t is the difference between the amount incorporated at prolonged incubation and the amount incorporated at time t . Incorporation was calculated from the specific radioactivity of $[\alpha\text{-}^{32}\text{P}]\text{dTTP}$.

Cross-Linking of Enzyme to Template-Primer and Determination of K_d for DNA. The cross-linking of enzyme to DNA was carried out as described previously (Pandey et al., 1994a,b). Primarily the 18/47 template-primer was used (see Chart 1) in this study; however, the results were also confirmed with two other self-annealing DNA of defined sequences (37-mer and 25-mer, Chart 1). The 5'-end-labeling of the 18-mer was performed using $[\gamma\text{-}^{32}\text{P}]\text{ATP}$ and T_4 polynucleotide kinase and purified by denaturing polyacrylamide gel electrophoresis, according to a standard protocol (Sambrook et al., 1989). The purified primer was appropriately diluted with unlabeled 18-mer and annealed to equimolar amounts of unlabeled 47-mer.

The determination of dissociation constants (K_d) for the enzyme-18/47 complex was carried out by UV-mediated cross-linking of 60 nM wild-type or mutant enzyme to variable concentrations of ^{32}P -18/47 (12–100 nM, 100 000 dpm/pmol), as described before (Pandey et al., 1994b).

Nucleotidyl Transferase Activity of the E-TP Complex. Nucleotidyl transferase activity of the enzyme containing covalently cross-linked template-primer was carried out as described previously (Pandey et al., 1994a). Fifteen picomoles of enzyme was cross-linked with 45 pmol of unlabeled TP in a standard irradiation mixture containing 50 mM HEPES, pH 8.0, 1 mM DTT, and 5 mM MgCl_2 in a final volume of 50 μL . The nucleotidyl transferase reactions were initiated by the addition of 50 μCi of complementary $[\alpha\text{-}^{32}\text{P}]\text{-dNTP}$ at 5 μM . The reaction was brought to completion by incubating at 25 °C for 20 min. Reactions were terminated by the addition of 1% SDS and 20 mM EDTA. Cross-linked species were resolved by SDS-PAGE, and radioactivity associated with the individual species was assessed by autoradiography, followed by determination of Cerenkov counts of the excised bands.

In order to show that the nucleotide addition to the cross-linked DNA was catalyzed by the enzyme species in the covalent complex and not by free enzyme, enzyme-TP covalent complexes were purified as follows: Scaled up (20 \times) irradiated samples were loaded on a DEAE-Sephadex column (1 mL) preequilibrated with 50 mM HEPES, pH 8.0, 1 mM DTT, 100 mM NaCl, and 5% glycerol (buffer A). Extensive washing with buffer A followed by washing with 350 mM NaCl in the same buffer removed the free enzyme. The enzyme-TP covalent complexes were then recovered by elution with 0.8 M NaCl in buffer A. The eluate was desalted and concentrated using Centriprep-30. The final preparation was free of un-cross-linked enzyme, as judged by the lack of activity on externally added synthetic template-primer. When un-cross-linked template-primer-enzyme complexes were processed through the same procedure, the entire enzyme activity was recovered in the 350 mM salt wash, while no detectable activity was associated with the 0.8 M eluent (data not shown). The details of these

Table 1: Kinetic Parameters of Wild-Type and Mutant Enzymes^a

| variable: saturating: | K_m (μM) | | | | k_{cat} (s^{-1}) | | |
|---|-------------------------|--------------|-------------|---------------------------|--------------------------------------|--------------|-------------|
| | dGTP rCdG | dGTP dCdG | TTP rAdT | dCdG ^b dGTP | dGTP rCdG | dGTP dCdG | TTP rAdT |
| WT | 3.0 | 1.7 | 3.5 | 0.09 | 0.27 | 1.40 | 1.1 |
| [Q151A] ^c | 4.1 | 31.7 | 8.0 | 0.10 | 0.02 | 0.26 | 0.01 |
| [Q151N] ^c | 2.8 | 2.8 | 5.1 | 0.09 | 0.25 | 1.50 | 1.0 |
| p66 _{WT} /p51 _{Q151A} | 2.9 | 2.0 | 3.5 | 0.10 | 0.30 | 1.55 | 1.3 |
| p66 _{Q151A} /p51 _{WT} | 3.6 | 28.2 | 5.0 | 0.11 | 0.03 | 0.30 | 0.01 |

^a Assays were performed as described in Methods. ^b A_{260} units/mL.

^c Mutations are in both subunits.

experiments, together with analysis of the DNA cross-linking sites in HIV-1 RT, will be published elsewhere (Pandey et al., in preparation).

Molecular Model of a Ternary HIV-1 RT/Template-Primer/dNTP Complex: Secondary Structure Prediction Studies. In order to assess the physicochemical contribution of Q151, we examined a ternary complex model of HIV-1 RT with template-primer and dNTP, built in our laboratory using the SYBYL 6.0 molecular modeling package, on an IRIS workstation (Yadav et al., unpublished results). The model contains a short DNA template-primer sequence (four template and three primer nucleotides) in the "A" conformation at overlapping positions with the DNA of the crystal structure (Jacobo-Molina et al., 1993). In addition, a substrate dNTP is docked in the model, in a manner that satisfies the following considerations (Yadav et al., unpublished results): (a) It forms hydrogen bonds with the corresponding template nucleotide, (b) it is in the same (A) conformation as the template-primer, and (c) the α -phosphorus of the docked TTP is oriented in the direction of the 3'-OH of the primer nucleotide, in such a manner as to facilitate a $\text{S}_{\text{N}}2$ nucleophilic attack by the 3'-OH (Pelletier et al., 1994; Sawaya et al., 1994).

Secondary structure predictions of the 11 reverse transcriptases were performed using a standard algorithm (CF) with the Mac Vector 4.0 software (supplied by Eastman-Kodak). The examined length was between residues 88 and 120 for HIV-1 RT; the corresponding areas for the other enzymes were derived from the alignment shown in Figure 3 of Boyer et al. (1992).

RESULTS

Overproduction and Purification of the Mutant and Wild-Type HIV-1 RTs. The recombinant clones containing wild-type HIV-1 RT and its two mutant derivatives Q151A and Q151N were grown, and the cell lysates were prepared as described in Methods. The HIV-1 RT proteins containing the hexahistidine region (His-tag) were selectively purified using metal-affinity chromatography. The wild-type HIV-1 RT prepared in this manner was mostly in the homodimer (p66/p66) form. Although this preparation displayed nearly identical kinetic parameters (Table 1) to those reported for recombinant HIV-1 RT by Chattopadhyay et al. (1992) and by Majumdar et al. (1988), we chose to prepare chimeric heterodimeric proteins as well, containing either the wild-type or the mutant residue on one of the polypeptides (p66_{WT}/p51_{Q151A} and p66_{Q151A}/p51_{WT}). We used these enzymes in order to confirm that p66 plays the dominant role in dNTP recognition (K_m) as well as in the nucleotidyl transferase reaction. In the case of mutant enzymes, the level of protein expression, solubility, yield, and the chromatographic char-

Chart 1: DNA Oligomers/TP Used

18 / 47 mer TP

CTT CCA TTC ACA CAG TGC -3'

GAA GGT AAG TGT GTC ACG ATG TCT GAC CTT GTT TTT GTG ACA TTG AG-5'

25 mer self annealing TP

```

      A   C
C      GAGTGGG-3'
T      CTCACCCAGAG-5'
      C   A

```

37 mer self annealing TP

CACGCAGTCTTCTCC-3'

TCACGTCAGAAGAGGATCCCTC-5'

acteristics were identical with those of the wild-type enzyme, suggesting that the substitution at position 151 did not cause any perturbation in the enzyme structure. In addition, the thermal denaturation profiles of the wild-type and mutant enzymes were nearly identical, as judged by the similar changes in polymerase activity upon incubation of enzyme protein at temperatures ranging from 25 to 60 °C (data not shown). Finally, energy calculation of HIV-1 RT containing substitutions at Q151 by the SYBYL molecular modeling program shows no major disturbance in the three-dimensional enzyme structure. The RNase H activities of the mutant and wild-type enzymes were the same (results not shown). These results suggest that the mutation did not significantly alter the overall conformation and tertiary folding of the enzyme molecule.

Determination of Steady-State Kinetic Constants. The effect of mutations at Q151 was assessed by the polymerase activity of the mutant enzymes using three different template-primers: namely, poly(rA)•(dT)₁₅, poly(rC)•(dG)₁₅, and poly(dC)•(dG)₁₅. The activity pattern and kinetic constants for each of the three template-primers were nearly identical for the wild-type and Q151N enzymes (Table 1). Q151A exhibited nearly complete loss of activity with poly(rA)•(dT)₁₅, with approximately 100-fold reduction in k_{cat} (Table 1). Interestingly, the polymerase activity of this mutant with poly(rC)•(dG)₁₅ or poly(dC)•(dG)₁₅ was less severely affected, with decrease in k_{cat} by approximately 15- and 5-fold, respectively. Since maximum activity of Q151A could be seen with poly(dC)•(dG)₁₅, further inhibition experiments were carried out using this template-primer. At saturating dGTP concentration, similar K_m s for poly(dC)•(dG)₁₅ were calculated for Q151A, Q151N, and wild-type enzyme, suggesting that there are no significant differences in the affinity of the mutant and control enzymes for this template-primer (Table 1). Similarly, determination of K_m s for dGTP with poly(rC)•(dG)₁₅ as the template-primer with all three enzymes showed no significant differences (Table 1). However, in the case of Q151A, a significant increase in K_m for dGTP was noted when poly(rC) template was replaced with poly(dC) template (Table 1).

Effect of the Mutation at Q151 on the Formation of the E-TP Binary Complex. The steady-state kinetic experiments suggested that replacement of Gln151 of RT had no effect on the ability of the enzyme to bind homopolymeric DNA. In order to confirm these results, and to extend them to heteropolymeric sequences, we performed binding studies by direct photochemical cross-linking of the enzymes with the 18/47 template-primer (Chart 1). The mobility of the labeled species, by means of SDS-PAGE, shows that the cross-linking is associated only with the p66 subunit (Figure 1, lanes 1–3). The specificity of the DNA cross-linking reaction at the active site of the enzymes was demonstrated

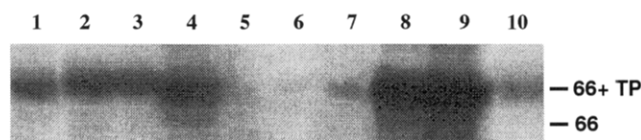


FIGURE 1: Cross-linking of ³²P-18/47 template-primer to the Q151 (wild type) and Q151N and Q151A mutant HIV-1 RTs and incorporation of [³²P]TTP to the E-TP covalent complexes. Enzyme-template-primer cross-linking reactions of wild-type (lane 1), Q151A (lane 2), and Q151N (lane 3) enzymes (both subunits mutated) were performed as described in Materials and Methods. Nucleotidyl transferase reactions involved cross-linking of 15 pmol of wild-type (lanes 4–6), Q151A (lane 7), Q151N (lane 8), p66_{WT}/p51_{Q151A} (lane 9), or p66_{Q151A}/p51_{WT} (lane 10) to 45 pmol of unlabeled 18/47, as above. After irradiation, 5 μM [³²P]TTP (50 μCi) and 5 mM MgCl₂ were added (except lane 5, where no MgCl₂ was added); the samples were incubated at room temperature for 20 min, and reactions were terminated by the addition of 1% SDS and 20 mM EDTA. Cross-linked species were resolved and processed as above. In lane 6, 5 μM [³²P]dGTP (mismatching nucleotide) (50 μCi) and 5 mM MgCl₂ were added.

by competitive reduction in cross-linking by the addition of poly(dC)•(dG)₁₅, but not by poly(dC) or oligo(dG)₁₅ alone, as described previously for the Klenow fragment (Pandey et al., 1994) (results not shown). The Scatchard plot of the ratio of cross-linked to free TP versus the concentration of cross-linked TP was linear, and the dissociation constants calculated from the slopes ($-1/K_d$) (Figure 2) were 8, 8, and 9 nM for the binding of 18/47 to [Q151A], [Q151N], and the wild-type enzymes, respectively. Similarly, the wild-type and mutant enzymes were found to have indistinguishable affinities for the 25-mer and 37-mer DNA template-primers (Chart 1), as well as for poly(rA)•(dT)₁₅ (results not shown). These results suggest that the mutation at Q151 does not affect the template-primer binding ability of HIV-1 RT.

Effect of the Mutation at Q151 on the Nucleotidyl Transferase Activity of the E-TP Covalent Complexes. The most compelling evidence for participation of Q151 in the substrate binding function is provided by the inability of only the Q151A-TP and not that of the wild-type or Q151N E-TP covalent complexes to catalyze an addition of dNTP. The specificity of the nucleotidyl transferase reaction is demonstrated by the ability of the wild-type E-18/47 covalent complex to add only [³²P]TTP (complementary nucleotide) (Figure 1, lane 4 vs lane 6) and not [³²P]dGTP (mismatching nucleotide; see Chart 1). Similarly, the wild-type E-25-mer covalent complex was able to add [³²P]dGTP (complementary nucleotide) and not [³²P]TTP (mismatching nucleotide; see Chart 1) (results not shown). Furthermore, the reaction is Mg²⁺-dependent (Figure 1, lane 4 vs lane 5). The amount of the E-TP covalent complex formed by the wild-type, Q151A, and Q151N enzymes is nearly identical, as seen in Figure 1, lanes 1–3. The control

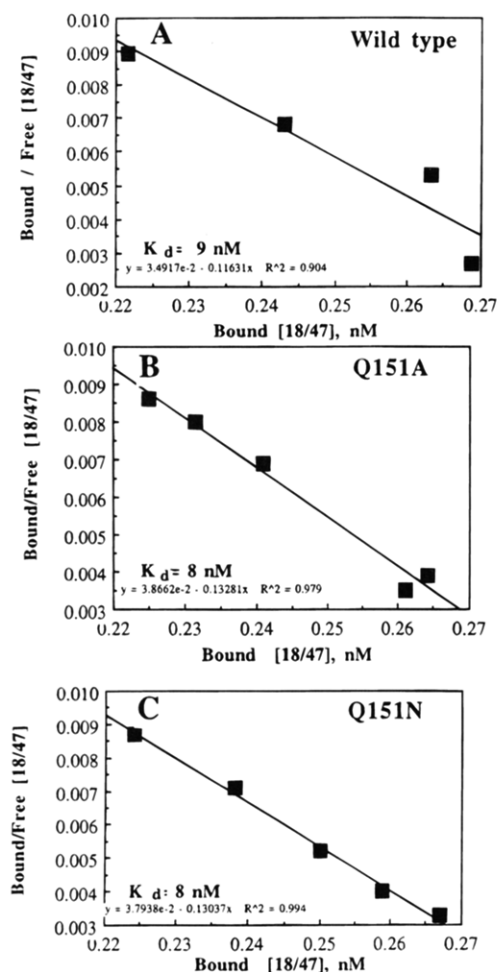


FIGURE 2: Scatchard plot of the quantity of enzyme–template-primer cross-linking as a function of TP concentration. Wild-type (A), Q151A (B), and Q151N (C) HIV-1 RT (60 nM) were incubated with varying concentrations of 5'-³²P-18/47-mer (12–100 nM) in a standard reaction mixture (50 μ L) and exposed to UV irradiation. The extent of cross-linking was determined as described in Methods. K_d s were calculated from the formula: slope = $-1/K_d$. Points in the graphs represent the mean values of duplicate samples. Standard error was <15%.

and two mutant enzymes also show similar K_d s for the 18/47-mer. Therefore, the addition of [α -³²P]dNTP onto the E–TP covalent complex is directly related to the ability of individual enzyme species to bind substrate and catalyze its addition. This function appears to be dramatically impaired for Q151A as compared to the wild-type enzyme (Figure 1, lanes 4 and 7). Furthermore, glutamine is required at the 151 position of only the p66 subunit, as the p66_{WT}/p51_{Q151A}–TP (Figure 1, lane 9) and not the p66_{Q151A}/p51_{WT} (Figure 1, lane 10) complex has nucleotidyl transferase activity. The conservative Q151N mutant complex exhibits the wild-type enzyme behavior (Figure 1, lane 8). These results strongly suggest that Q151 is involved in the substrate binding function.

Rates of the First Nucleotide Incorporation by the Wild-Type and Mutant Enzymes. The unaltered ability of Q151A for binding to DNA template-primer indicates that Q151 participates at a reaction step following DNA binding. Such steps, in sequential order, are (1) binding of dNTP and formation of the activation complex, (2) removal of the PP_i product, and (3) translocation of the enzyme along the elongated template-primer. Since the binding of the first nucleotide is independent of steps 2 and 3, the single nucleotide addition can be used to determine if the reaction

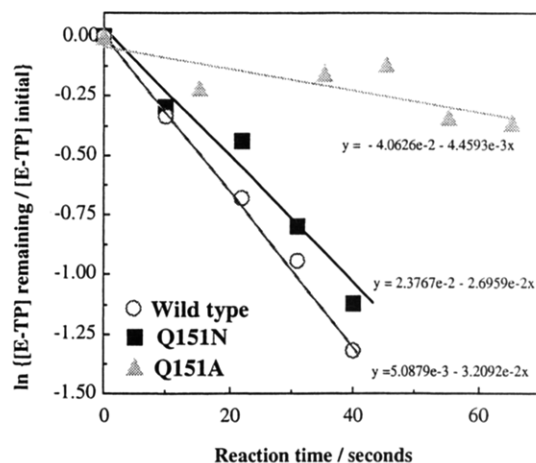


FIGURE 3: Rate of first nucleotide incorporation by wild-type, Q151N, and Q151A HIV-1 RTs. The rate of incorporation of the first nucleotide was measured by monitoring the incorporation of [α -³²P]TMP into an 18/47-mer template-primer in a standard reaction mixture, as described in Methods. The first-order rate of single nucleotide incorporation was then calculated as detailed in Methods. Open circles, filled squares, and filled triangles represent values for the wild-type, Q151N, and Q151A HIV-1 RT enzymes, respectively.

is affected at the level of dNTP binding. As shown in Figure 3, the addition of the first nucleotide by Q151A is severely reduced (nearly 70-fold) as compared to the wild-type enzyme. These results are consistent with those of the kinetic analysis (Q151A showing increased K_m for dNTP) and those of the nucleotidyl transferase experiments, suggesting involvement of the Q151 residue in as early in the mechanism as in the dNTP binding function and/or stabilization of the transition-state complex.

Effect of Mutation on the Divalent Cation Preference by HIV-1 RT. Additional evidence for the role of Q151 in the substrate binding function was provided by the changes in metal ion requirement of the Q151A mutant enzyme. HIV-1 RT, similar to many other polymerases, is known to require divalent cation for activity. Although the metal ion of preference in the case of HIV-1 RT is Mg²⁺, other cations such as Mn²⁺ can also support catalysis, although less efficiently. The metal preference may depend on the ability of an individual enzyme to bind the dNTP–metal complex and utilize it to stabilize the transition state of the reaction. Therefore, such preferences are likely to be affected upon subtle variation in the conformation of the substrate binding site. As shown in Figure 4, the wild-type HIV-1 RT shows a preference for Mg²⁺ cation, but the Q151A mutant exhibits alteration in its metal ion requirement. It is able to utilize Mn²⁺ at a Mn/Mg activity ratio up to ~70 times higher than the wild-type enzyme (Figure 4A,C). The conservative Q151N mutant appears to have retained the metal preference pattern which is closer to the wild-type enzyme, yet with persistent small changes. This unusual preference of Q151A for Mn²⁺ may also be suggestive of a role for Q151 in the substrate binding function.

Molecular Modeling Studies. The molecular model used was based on the C- α coordinates of the crystal structure of the HIV-1 RT–DNA complex (Yadav et al., unpublished results; Jacobo-Molina et al., 1993). It is, therefore, limited in its accuracy by at least the 3.0 Å resolution limit of the crystal structure coordinates. In addition, it is not meant to substitute the crystal structure results but to be used tentatively in the analysis of mutagenesis results, until the

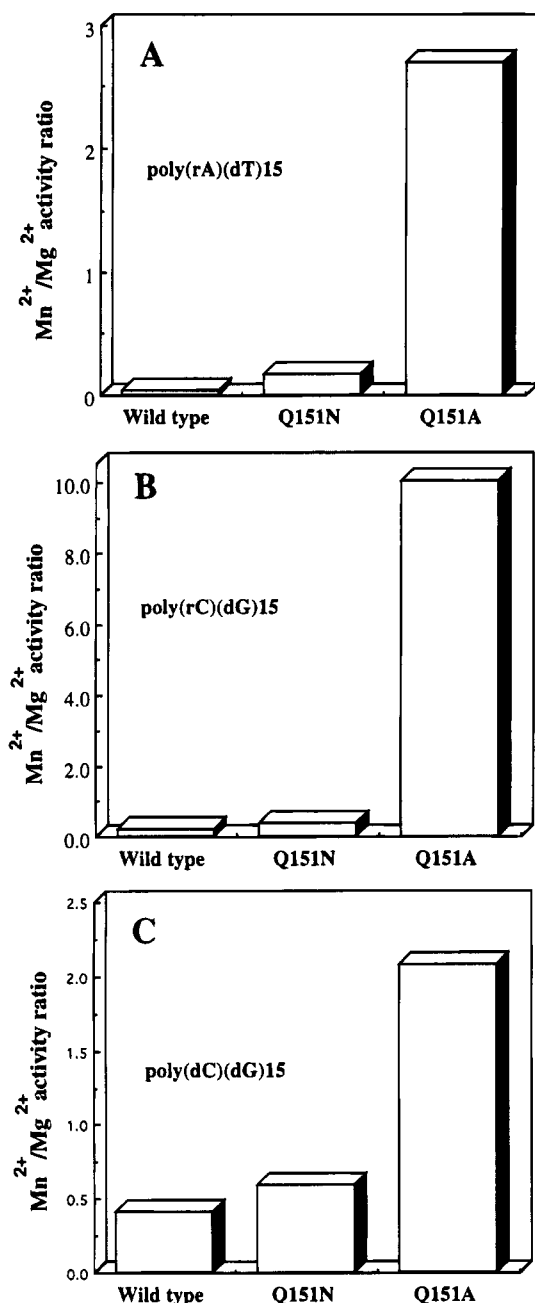


FIGURE 4: Divalent cation preference of Q151 (wild type), Q151N, and Q151A HIV-1 RTs. The polymerase activity on poly(rA)(dT)₁₅ (A), pol (rC)(dG)₁₅ (B), and poly(dC)(dG)₁₅ (C) template-primers was measured as described in Methods with 30 ng of wild-type, 30 ng of Q151N, and 120 ng of Q151A HIV-1 RTs in the presence of Mn²⁺ (0.4 mM) and Mg²⁺ (5 mM). The ratio of activities with the three template-primers in the presence of Mn²⁺ to that in the presence of Mg²⁺ is indicated for the three enzymes.

full coordinates of the complex are available. In Figure 5, the structure of selected amino acids of the pretransition-state complex is shown. The position of the incoming substrate TTP satisfies the requirement for hydrogen bond formation with the template nucleotide. In addition, the α -phosphate group is poised to undergo nucleophilic attack by the 3'-OH of the primer strand. The β - and γ -phosphate arch is similar to the one observed in the crystal structure of β -pol (Pelletier et al., 1994), positioning it in the vicinity of the catalytic triad of aspartates (110, 185, and 186). This arrangement allows for bridging interactions (not shown) with the two Mg²⁺ ion(s), transferred from the β -pol structure (Pelletier et al., 1994). The position of the β -phosphate

substructure of TTP is close to Arg72, which has been proposed to be the PP_i acceptor residue in HIV-1 RT (Sarafianos et al., 1994, unpublished results). The side chain of Q151 of the p66 subunit in this complex points toward the base part of the substrate and its complementary template nucleotide (Figure 5). The amide hydrogens of Q151 may be interacting (3–4 Å) with the H-bond acceptor of the base moiety of the dNTP substrate (either with the carbonyl oxygen in the C2 position of a pyrimidine ring or with the free pair of electrons of the N3 of purines) (3–4 Å). In our molecular model, the amide hydrogens of Q151 are also proximal to the H-bond acceptor of the base moiety of the template nucleotide complementary to the dNTP substrate (either with the carbonyl oxygen in the C2 position of a pyrimidine ring or with the free pair of electrons of the N3 nitrogen of purines) (3–4 Å). Therefore, it is possible that Q151 confers the changes in dNTP binding properties indirectly, i.e., via interactions with the complementary template nucleotide. However, we tend to discount that possibility, as the template-primer binding ability of Q151A and the wild-type enzyme is indistinguishable. At this point we cannot exclude the possibility of additional or different interactions of Q151 with other parts of dNTP, such as the ribose base (3–5 Å). However, we can confidently assert that Q151 is too distant to have any direct interactions with the β - and γ -phosphate groups of dNTP.

The amide oxygen of Q151 is proximal to the guanidino group of Arg72 (~3 Å, Figure 5), possibly stabilizing the Arg72 residue and indirectly aiding the removal of the pyrophosphate product. Such an interaction is in agreement with our observed moderate resistance of Q151A to PFA (IC₅₀ increase from 17 to 41 μ M): In the absence of Q151, the guanidino hydrogens of Arg72 may not be positioned properly to remove pyrophosphate and/or bind its analog (PFA) effectively. As expected, the Q151 of the p51 subunit is distant from the HIV-1 RT active site (results not shown).

pH Dependence of the Wild-Type and Mutant Enzyme Activities. In order to detect possible differences in the ionization of the amino acid side chains involved in the catalytic activities of the wild-type and mutant enzymes, we determined their kinetic constants at various pHs. The results show that the impairment of the Q151A mutation can be overcome at high pH (Figure 6). For the wild-type HIV-1 RT the optimal activity pH is at approximately 8. At higher pH the polymerase activity of the wild-type enzyme is decreased. Interestingly, Q151N has two activity optima for its polymerase activity, one identical to the wild-type enzyme at pH ~8 and a second one at higher pH (Figure 6). This is probably due to a titration of an unknown residue (possibly lysine) that is either (a) not accessible for titration in the wild-type enzyme or (b) even when titrated, does not switch the reaction to a different type of mechanism (involving basic interactions). Surprisingly, Q151A is able to catalyze polymerization more efficiently than the wild-type enzyme at high pH (Figure 6). In order to examine the nature of the changes at different pHs, we determined the K_m s of the wild-type and Q151A mutant enzymes at different pHs. The results suggest that the activation of Q151A occurs through an improvement in both dNTP binding and catalysis (concurrent increase in k_{cat} and decrease in K_m , Table 2). These changes indicate the versatility of the enzyme to catalyze DNA synthesis, presumably by employing different mechanisms. The possibility of the base part of dNTP being titrated at high pH adds to the difficulties of interpreting the

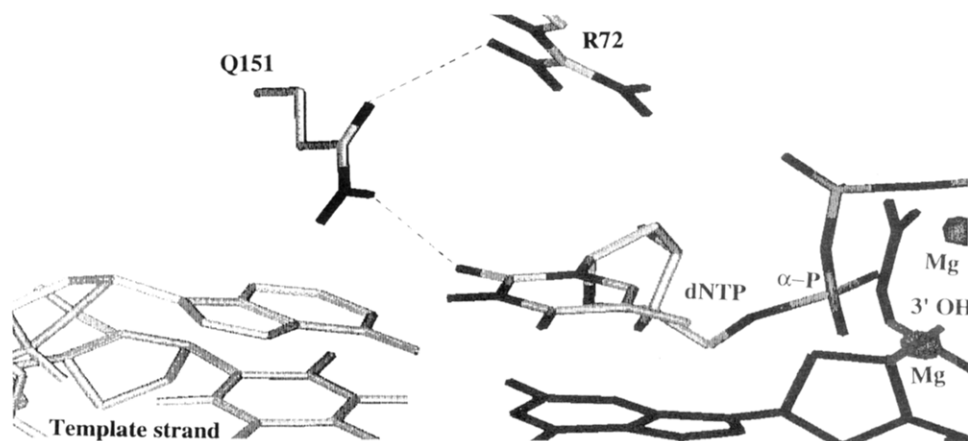


FIGURE 5: A model of the substrate binding region of HIV-1 RT and suggested role for Q151. The model was adapted from Yadav et al. (unpublished) and built as described in Methodson the basis of the C- α crystal structure coordinates (Jacobo-Molina et al., 1993). Two nucleotides of the template strand are shown at the lower left part of the figure. The incoming substrate dNTP molecule is shown in H-bond position with the complementary template nucleotide. The guanidino hydrogens of Arg72 are at a $\sim 2\text{--}3$ Å distance from the amide oxygen of Gln151. The amide hydrogens of Q151 are at a $\sim 3\text{--}4$ Å distance from the C2 carbonyl oxygen of dNTP. Notice that all four nucleotides have a H-bond acceptor in their equivalent positions (Scheme 1B). The oxygens of the β -phosphate of dNTP are at a $\sim 3\text{--}4$ Å distance from the guanidine group of Arg72. For the sake of clarity, some amino acids interfering with the view are omitted.

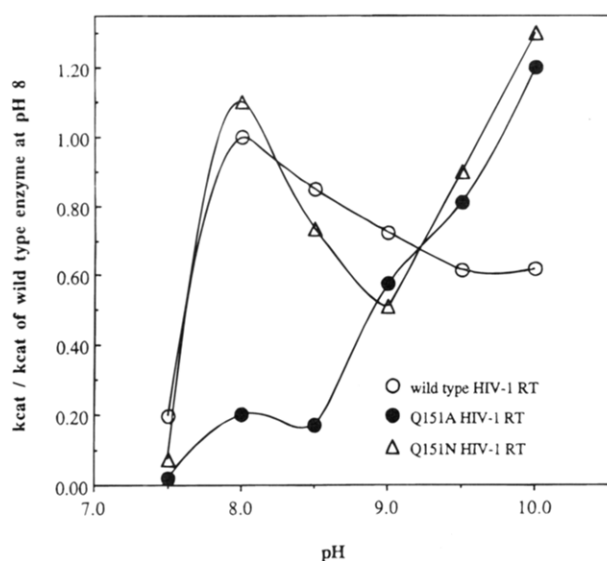


FIGURE 6: Effect of pH on the activity of the wild-type and mutant HIV-1 RTs. The standard reactions containing poly(dC) \cdot (dG) $_{15}$ as template-primer and dGTP as substrate were carried out at the indicated pH of the reaction mixture. The pH adjustments were made using glycine buffers. Triplicate samples, for five different dGTP concentrations, were assayed for each pH value and for every protein. The results were used to calculate graphically the k_{cat} and K_m values from standard Lineweaver–Burk plots (plots not shown). The ratio of k_{cat} values for individual enzymes at various pHs to that observed with the wild-type enzyme at pH 8.0 is plotted.

Table 2: Effect of pH on the K_m for dGTP in HIV-1 RT^a

| pH | K_m (μM) | |
|----|-------------------------|-------|
| | wild type | Q151A |
| 8 | 1.8 | 31 |
| 9 | 1.3 | 6 |
| 10 | 1.8 | 7 |

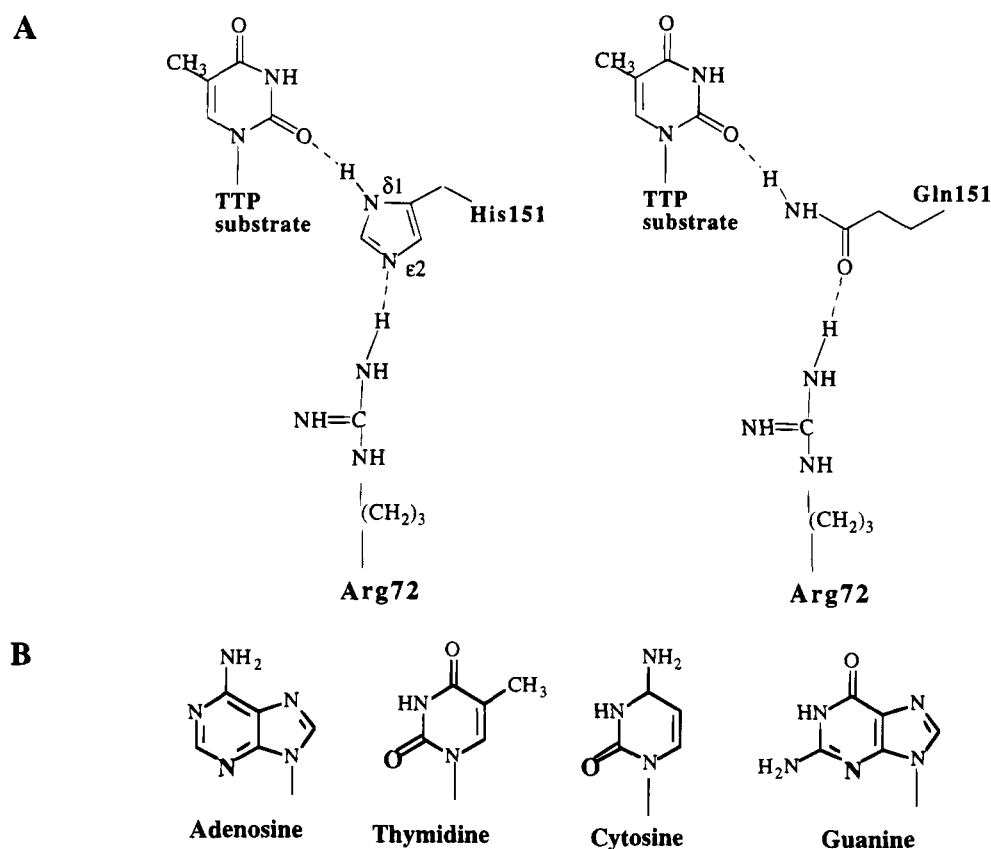
^a Polymerase assays were carried out in standard reaction mixtures adjusted to the desired pH, with poly(dC) \cdot (dG) $_{15}$ as the template-primer and dGTP as the variable substrate.

results of the pH experiments. However, the conclusion remains that Q151A at high pH is able to overcome its catalytic deficiency and polymerize even more efficiently than the wild-type enzyme.

DISCUSSION

Detailed knowledge of the active site geometry as well as of the catalytic mechanism of the HIV-1 RT enzyme is a prerequisite for rational drug design. Despite the availability of the crystal structure of HIV-1 RT (Jacobo-Molina et al., 1993; Kohlstaedt et al., 1992) and numerous mutational studies, the specific residues that are part of the substrate binding site and their role in the catalytic mechanism have not yet been clarified. This is partly due to the incomplete characterization of the mutant species with regard to the polymerization mechanism. As part of our laboratory's efforts to systematically address the structure–function relationship in various DNA polymerases, Yadav et al. (1994) showed that 10 residues of the Klenow fragment of *E. coli* DNA polymerase I have equivalent counterparts in the three-dimensional structure of the catalytic domain of HIV-1 RT, suggesting a functional equivalence of these residues. N845 of the Klenow fragment was one of the 10 residues that has been characterized through site-directed mutagenesis studies (Polesky et al., 1990). These studies suggested that N845 of the pol I enzyme is involved in the process of dNTP binding. Since, in HIV-1 RT, Q151 is the proposed counterpart of N845, we investigated the role of Q151 in the catalysis of DNA synthesis by HIV-1 RT. In order to obtain experimental evidence, we constructed and extensively characterized HIV-1 RTs with conservative and nonconservative mutations at Q151. In addition, we prepared chimeric reconstituted enzymes, with the Q151 residue selectively mutated to Ala in one of the two subunits. Incidentally, a mutant of HIV-1 RT at this position had been constructed previously with substitution of His for Gln. Such a mutation may be considered conservative, given the structural similarity as well as the potential for hydrogen bond formation by the two residues, as shown in Scheme 1. A moderate reduction in the polymerase activity of the mutant HIV-1 RT in crude cell extracts was reported, without any further investigation of the role of this residue in the catalytic function (Larder et al., 1989b).

Our results show that the Q151 residue of only the p66 subunit is necessary for efficient polymerization. The Q151A mutant (mutation in both subunits) was almost inactive ($<2\%$ of the wild-type activity) on the poly(rA)-

Scheme 1^a

^a The ability of histidine to act as a hydrogen bond acceptor (through its $\epsilon 2$ nitrogen) and as a hydrogen bond donor (through its $\delta 1$ amine hydrogen) at the same time parallels that of glutamine, which through its amide group can also perform both functions. Notice that dCTP could act similarly as a hydrogen bond acceptor, whereas dATP and dGTP would interact through their basic N3 nitrogen (bold letters in part B).

(dT)₁₅ template-primer (Table 1). When the mutation was introduced selectively in the p51 subunit, the resulting enzyme (p66_{WT}/p51_{Q151A}) had activity similar to that of the wild-type enzyme (Table 1, Figure 1). On the other hand, the kinetic parameters of p66_{Q151A}/p51_{WT} are indistinguishable from those of the enzyme mutated in the both subunits (Table 1, Figure 1). The catalytic properties of Gln151 could be fully compensated by Asn, as Q → N mutation had no effect on the polymerase function (Table 1). These results suggest that the involvement of Q151 in catalysis is through the p66 subunit, probably via its hydrogen bond forming capability.

We have shown that Q151 does not participate in the process of DNA binding, as the K_m and K_d for the DNA template-primer of Q151A were comparable to those of the wild-type enzyme (Figures 1 and 2 and Table 1). Thus, the defect in the polymerase reaction catalyzed by the mutant enzyme and presumably the functional role of Gln151 appear to lie at a reaction step beyond the E-TP complex formation. A substantial increase in the K_m for dNTP with DNA template by substitution of Q → A (Table 1) suggested a possible involvement of Q151 in the binding of dNTP. However, no effect on the binding/affinity of dNTP substrates was observed with RNA templates. Similar template-primer-specific effects of mutations as well as of some inhibitors on the polymerase activity of HIV and other enzymes have been reported previously (Pandey et al., 1994b; Desai et al., 1994; Polesky et al., 1992; Tramontano & Cheng, 1992; Sarafianos et al., unpublished observations). It is therefore reasonable to assume that Q151 may have different roles with DNA and RNA templates. For example, with DNA templates it may be participating in the dNTP binding, although an additional involvement at the catalytic step

cannot be excluded. In the case of RNA templates, it could have a role in either the catalytic (chemical) or pyrophosphate binding/translocation steps. However, the latter possibility seems unlikely, as we have noted similar reductions in the rate of first and second nucleotide addition on poly(rA)·(dT)₁₅ (unpublished observations). These results are not consistent with the defect in pyrophosphate removal or the subsequent translocation step. As a crystal structure of HIV-1 RT complexed with RNA-DNA template-primer is not available, it would not be possible to speculate the precise role of Q151 with RNA templates through the molecular modeling techniques.

An increase in K_m for dNTP was reported for the N845A mutant of the Klenow fragment, with only one template primer examined (Polesky et al., 1990). These results led to the conclusion that N845 (the counterpart of the Klenow fragment to the Q151 residue in the HIV-1 RT enzyme) participates at the binding of dNTP. However, the measured K_m is an apparent kinetic constant, and a function of multiple reaction steps, thus providing only general mechanistic information. As our objective was to pinpoint the specific role of Q151 in the catalytic mechanism, we determined first-order kinetics of a single nucleotide addition by the enzyme. The rate of the first nucleotide addition can be affected only by changes in the DNA or dNTP binding and not by defects at subsequent reaction steps, such as PP_i removal or translocation along the template-primer. The latter was the case with R72 of HIV-1 RT, which appears to participate in the PP_i removal and thus has minimal effect in the rate of the first nucleotide addition by R72A (Sarafianos et al., unpublished results). Our results show that the rate of the first nucleotide addition by Q151A is severely affected,

suggesting an effect in the reaction mechanism, as early as in the dNTP binding step.

We report here that WT enzyme covalently cross-linked with the DNA–DNA template primer is able to catalyze the addition of one nucleotide onto the immobilized template-primer without being able to translocate along the template strand. This addition reaction is metal dependent and specific to the complementary nucleotide, as mismatched dNTP is not used as the substrate (Figure 1, lanes 5 and 6). These results with the WT enzyme strongly suggest that the dNTP binding pocket remains unaffected upon covalent cross-linking of the template-primer to the enzyme. Therefore, this technique is able to assess reliably the substrate binding ability of HIV-1 RT. As the yield of E–TP covalent complex formation is the same for the wild-type and the mutant enzymes (Figure 1, lanes 1–3, Figure 2, and Table 1), including the reconstituted chimeric species (results not shown), the ability of only the Q151A–DNA complex (and not that of Q151N or the wild-type enzyme) to add a nucleotide is significantly reduced. Furthermore, this impairment is associated with mutation only in the p66 subunit. These experiments provide compelling evidence for the involvement of Q151 of the p66 subunit in the substrate binding function, in the context of the ternary complex.

Further corroborating evidence for the dNTP binding role of Q151 was provided by the alteration in the divalent cation preferences by Q151A. As the preferred divalent metal ion binding, in this case Mg^{2+} , occurs at the substrate binding site (Sawaya et al., 1994), it is expected that any direct or indirect distortion of this site could affect the divalent cation specificity of the enzyme. Our results show dramatic changes in the metal preference of the mutant enzyme (Q151); the Mg/Mn activity ratio was up to 70 times higher for Q151A, as compared to the wild-type enzyme (Figure 4). Considerably smaller changes (up to 7 times) have been reported for another HIV-1 RT mutant (E89G). Crystallographic (Jacobo-Molina et al., 1993; Kohlstaedt et al., 1992) and molecular modeling data (unpublished observations in our laboratory) suggest that the E89 residue of HIV-1 RT is not at the substrate binding pocket but at a position to affect the DNA binding (unpublished observations in our laboratory). However, the mutation at position 89 of the p66 HIV-1 RT subunit influences (apparently indirectly) the substrate binding site, as evidenced by an increase in K_m for dNTP, as well as the PFA and ddTTP resistance characteristics of the E89G mutant (Kew et al., 1994). As the template-primer participates in the substrate binding through H-bond interaction of the template base to dNTP (Majumdar et al., 1988), it is possible that changes in the DNA binding site induced upon E89G mutation are translated through the template strand to the dNTP binding site and thereby moderately affect the metal specificity of the E89G mutant along with other substrate binding characteristics. Unfortunately, no data are available on the DNA binding ability of E89G for direct comparison with Q151A. However, the kinetic (Table 1), cross-linking (Figure 1, lanes 1–3, Figure 2), and molecular modeling (Figure 5) evidence presented in this work strongly suggests that the participation of Q151 of the p66 subunit in the mechanism of HIV-1 RT is not through DNA binding. In addition, the dramatic metal preference changes observed with the Q151A mutant are also consistent with a direct interaction of Q151 at the dNTP binding site.

Table 3: Amino Acid Sequence Comparison between HIV-1 RT and Reverse Transcriptases from Other Sources^a

| | | | | | |
|--------------------------|-------|----------|------------|-------|-------|
| HIV-1 (147–157) | ...NV | L | PQG | WKG | SP... |
| BLV (138–148) | ...RV | L | PQG | F I N | SP... |
| CAEV (138–148) | ...KV | L | PQG | WKL | SP... |
| EIAV (341–351) | ...KC | L | PQG | FVL | SP... |
| HTLV-I (161–171) | ...KV | L | PQG | FKN | SP... |
| HTLV-II (246–256) | ...TV | L | PQG | FKN | SP... |
| MMTV (140–150) | ...RV | L | PQG | WKN | SP... |
| MoMLV (316–326) | ...TR | L | PQG | FKN | SP... |
| MPMV (169–179) | ...KV | L | PQG | WAN | SP... |
| RSV (153–163) | ...KC | L | PQG | WKL | SP... |
| VISNA (296–306) | ...KV | L | PQG | WKL | SP... |

^a The sequence alignment shown here is taken from Figure 3 in Boyer et al. (1993). Amino acid numbering is shown in parentheses. Amino acids conserved in all sequences are shown in bold type. Notice the conservation of the LPQG sequence which starts a common secondary structure element (turn) for all enzymes (see Discussion). Abbreviations: BLV, bovine leukemia virus; CAEV, caprine arthritis encephalitis virus; EIAV, equine infectious anemia virus; HTLV-I and -II, human T-cell leukemia virus types I and II; MMTV, mouse mammary tumor virus; MoMLV, Moloney murine leukemia virus; MPMV, Mason-Pfizer monkey virus; RSV, Rous sarcoma virus; VISNA, visna virus.

We observed only a moderate resistance of Q151A to PFA (IC_{50} increased from 17 to 41 μM). Although the exact mechanism of PFA resistance is not entirely known, the existing kinetic data (Abbotts et al., 1988) suggest that PFA binds at the PP_i binding subdomain of the dNTP binding site. Arg72 of HIV-1 RT has been proposed as the binding/acceptor residue of the leaving PP_i product, and the R72A mutant has a complete resistance to PFA (Sarafianos et al., unpublished). Our working computer-assisted molecular model of HIV-1 RT is consistent with these data, showing Arg72 at a ~ 4 Å distance from the β -phosphate of the substrate dNTP. Interestingly, although the side chain of Q151 (Figure 5) seems to be prohibitively far to interact directly with the leaving PP_i (Figure 5), the Q151 amide oxygen appears to be poised for interaction with the Arg72 guanidine hydrogens (Figure 5, ~ 3 Å distance). Such an interaction may contribute to the stabilization of the Arg72 position, indirectly aiding in the removal/binding of PP_i. This contention would explain the relatively weak resistance of Q151A to PFA. We should mention that this model was built on the basis of the coordinates of a crystal structure with a resolution of 3.0 Å (Jacobo-Molina et al., 1993; Yadav et al., unpublished results). Consequently, the evaluation of distances in Figure 5 is subject to this limitation as well until a crystal structure with higher resolution is solved. As it stands now, the most likely interaction of the side chain of Gln151 is with the base moiety of dNTP, as shown in Figure 5; such an interaction is consistent with our experimental results, as it would help to stabilize the substrate in a position that allows for the H-bond interaction with the complementary template. However, it is possible that different H-bonding patterns may emerge, depending on the orientation of the individual dNTP base. A crystal structure of a ternary complex (HIV-1 RT/template-primer/dNTP), similar to the one of β -pol (Pelletier et al., 1994), would confirm any specific interactions of dNTP at the active site.

Although N845 of the Klenow fragment and Q151 of HIV-1 RT seem to be spatially and functionally homologous, they are part of different secondary structure elements: N845 is part of an α -helix (Q), whereas Q151 is located on a turn, preceded by Leu149 and Pro150 and followed by Gly152

(Table 3), a constellation of residues diagnostic of secondary structure changes. Pro150 is conserved in all RNA-dependent DNA polymerases and Gln151 along with Gly152 in all reverse transcriptases [Table 3 and Jacobo-Molina and Arnold (1991)]. Site-specific mutagenesis on Pro150 resulted in complete loss of activity (Boyer et al., 1992). Interestingly, our secondary structure prediction studies for all 11 reverse transcriptases in Table 3 assign Pro150 and Gln151 to be at the beginning of a turn. On the basis of the above, we propose here that the role of Pro150 is to contribute to the formation of this vital turn; by doing so, the side chain of Gln151 is placed in position at the substrate binding site. It is, therefore, expected that the corresponding glutamines in the other reverse transcriptases have similar roles in the catalytic mechanisms of the corresponding enzymes. The above hypothesis has yet to be tested in the other enzymes listed in Table 3.

In conclusion, we have presented here strong experimental and computer modeling evidence that places the Q151 residue of the p66 subunit at the substrate binding site of HIV-1 RT.

ACKNOWLEDGMENT

We are thankful to Dr. Prem Yadav for giving us early access to his prepolymerase HIV-1 RT molecular model.

REFERENCES

- Abbotts, J., SenGupta, D. N., Zon, G., & Wilson, S. H. (1988) *J. Biol. Chem.* 263, 15094–15103.
- Abbotts, J., Bebenek, K., Kunkel, T., & Wilson, S. H. (1993) *J. Biol. Chem.* 268, 10312–10323.
- Ausubel, F. M., Brent, R., Kingston, R. E., Moore, D. D., Seidman, J. S., Smith, J. A., & Struhl, K. (1987) *Current Protocol in Molecular Biology*, Greene Publishing Associates and Wiley-Interscience, John Wiley & Sons, New York.
- Basu, A., & Modak, M. J. (1987) *Biochemistry* 26, 1704–1709.
- Basu, A., Tirumalai, R. S., & Modak, M. J. (1989) *J. Biol. Chem.* 264, 8746–8752.
- Beard, W. A., Stahl, S. J., Kim, H. R., Bebenek, K., Kumar, A., Strub, M. P., Beccera, S. P., Kunkel, T. A., & Wilson, S. H. (1994) *J. Biol. Chem.* 269, 28091–28097.
- Beese, L. S., Friedman, J. M., & Steitz, T. A. (1993) *Biochemistry* 32, 14095–14101.
- Boyer, P. L., Ferris, A. L., & Hughes, S. H. (1992) *J. Virol.* 66, 1031–1039.
- Boyer, P. L., Ferris, A. L., & Hughes, S. H. (1992) *J. Virol.* 66, 7533–7537.
- Boyer, P. L., Ferris, A. L., Clark, P., Whitmer, J., Frank, P., Tantillo, C., Arnold, E., & Hughes, S. H. (1994) *J. Mol. Biol.* 243, 472–483.
- Chattopadhyay, D., Evans, D. B., Deibel, M. R., Vosters, A. F., Eckenrode, F. M., Einspahr, H. M., Hui, J. O., Tomaselli, A. G., Zurcher-Neely, H. A., Heinrikson, R. L., & Sharma, S. K. (1992) *J. Biol. Chem.* 267, 14227–14232.
- Cheng, N., Merrill, B. M., Painter, G. R., Frick, L. W., & Furman, P. A. (1993) *Biochemistry* 32, 7630–7634.
- Cleland, W. W. (1963) *Biochim. Biophys. Acta* 67, 104–137.
- Desai, S. D., Pandey, V. N., & Modak, M. J. (1994) *Biochemistry* 33, 11868–11874.
- Hizi, A., Barber, A., & Hughes, S. H. (1989) *Virology* 170, 326–329.
- Hizi, A., Hughes, S. H., & Arnold, E. (1993) *Proc. Natl. Acad. Sci. U.S.A.* 90, 6320–6324.
- Jacobo-Molina, A., & Arnold, E. (1991) *Biochemistry* 30, 6351–6356.
- Jacobo-Molina, A., Ding, J., Nanni, R. G., Clark, A. D., Lu, X., Tantillo, C., Williams, R. L., Kamer, G., Ferris, A. L., Clark, P., Hizi, A., Hughes, S. H., & Arnold, E. (1993) *Proc. Natl. Acad. Sci. U.S.A.* 90, 6320–6324.
- Jacques, P. S., Wohrl, B. M., Ottmann, M., Darlix, J. L., & Le Grice, S. F. J. (1994) *J. Biol. Chem.* 269, 26472–26478.
- Kew, Y., Qingbin, S., & Prasad, V. R. (1994) *J. Biol. Chem.* 269, 15331–15336.
- Kohlstaedt, L. A., Wang, J., Friedman, J. M., Rice, P. A., & Steitz, T. A. (1992) *Science* 256, 1783–1790.
- Kunkel, T. A., Roberts, J. D., & Zakour, R. A. (1987) *Methods Enzymol.* 154, 367–382.
- Larder, B. A. (1993) *Reverse Transcriptase* (Skalka, A. M., & Goff, S. P., Eds.) pp 205–222, Cold Spring Harbor Laboratory Press, Cold Spring Harbor, NY.
- Larder, B. A., & Kemp, S. D. (1989) *Science* 246, 1155–1158.
- Larder, B. A., Purifoy, D. J. M., Powell, K. L., & Darby, G. (1987) *Nature* 327, 716–717.
- Larder, B. A., Darby, G., & Richman, D. D. (1989a) *Science* 243, 1731–1734.
- Larder, B. A., Kemp, S. D., & Purifoy, D. J. M. (1989b) *Proc. Natl. Acad. Sci. U.S.A.* 86, 4803–4807.
- Larder, B. A., Kellam, P., & Kemp, S. D. (1991) *AIDS* 5, 137–144.
- LeGrice, S. F. J., Naas, T., Wohlgensinger, B., & Schatz, O. (1991) *EMBO J.* 10, 3905–3911.
- Lowe, D. M., Parmar, V., Kemp, S. D., & Larder, B. A. (1991) *FEBS Lett.* 282, 231–234.
- Majumdar, C., Abbotts, J., Broder, S., & Wilson, S. H. (1988) *J. Biol. Chem.* 263, 15657–15665.
- Pandey, V. N., Stone, K. L., Williams, K. R., & Modak, M. J. (1987) *Biochemistry* 26, 7744–7748.
- Pandey, V. N., Kaushik, N. A., Sanzgiri, R. P., Patil, M. S., & Barik, S. (1993) *Eur. J. Biochem.* 214, 59–65.
- Pandey, V. N., Kaushik, N., & Modak, M. J. (1994a) *J. Biol. Chem.* 269, 21828–21834.
- Pandey, V. N., Kaushik, N., & Modak, M. J. (1994b) *J. Biol. Chem.* 269, 13259–13265.
- Pelletier, H., Sawaya, M. R., Kumar, A., Wilson, S. H., & Kraut, J. (1994) *Science* 264, 1891–1903.
- Polesky, A. H., Steitz, T. A., Grindley, N. D. F., & Joyce, C. M. (1990) *J. Biol. Chem.* 265, 14579–14591.
- Prasad, V. R., & Goff, S. P. (1989) *Proc. Natl. Acad. Sci. U.S.A.* 86, 3104–3108.
- Prasad, V. R., Lowy, I., de los Santos, T., Chiang, L., & Goff, S. P. (1991) *Proc. Natl. Acad. Sci. U.S.A.* 88, 11363–11367.
- Sambrook, J., Fritsch, E. F., & Maniatis, T. (1989) *Molecular Cloning*, pp 5.68–5.72, Cold Spring Harbor Laboratory Press, Cold Spring Harbor, NY.
- Sawaya, M. R., Pelletier, H., Kumar, A., Wilson, S. H., & Kraut, J. (1994) *Science* 264, 1930–1935.
- Setlow, P., Brutlag, D., & Kornberg, A. (1972) *J. Biol. Chem.* 247, 224–231.
- Shafer, R. W., Kozal, M. J., Winters, M. A., Iversen, A. K. N., Katzenstein, D. A., Ragni, M. V., Meyer, W. A., III, Gupta, P., Rasheed, S., Coombs, R., Katzman, M., Fiscus, S., & Merigan, T. C. (1994) *J. Infect. Dis.* 169, 722–729.
- Sharma, S. K., Evans, D. B., Vosters, A. F., McQuade, T. J., & Tarpley, W. G. (1991) *Biotechnol. Appl. Biochem.* 14, 69–81.
- Tantillo, C., Ding, J., Jacobo-Molina, A., Nanni, R. G., Boyer, P. L., Hughes, S. H., Pauwels, R., Andries, K., Janssen, P. A. J., & Arnold, E. (1994) *J. Mol. Biol.* 243, 369–387.
- Tramontano, E., & Cheng, Y., (1992) *Biochem. Pharmacol.* 43, 1371–1376.
- Yadav, P. N. S., Yadav, J. S., Arnold, E., & Modak, M. J. (1994) *J. Biol. Chem.* 269, 716–720.